

LETTERS

The increasing intensity of the strongest tropical cyclones

James B. Elsner¹, James P. Kossin² & Thomas H. Jagger¹

Atlantic tropical cyclones are getting stronger on average, with a 30-year trend that has been related to an increase in ocean temperatures over the Atlantic Ocean and elsewhere^{1–4}. Over the rest of the tropics, however, possible trends in tropical cyclone intensity are less obvious, owing to the unreliability and incompleteness of the observational record and to a restricted focus, in previous trend analyses, on changes in average intensity. Here we overcome these two limitations by examining trends in the upper quantiles of per-cyclone maximum wind speeds (that is, the maximum intensities that cyclones achieve during their lifetimes), estimated from homogeneous data derived from an archive of satellite records. We find significant upward trends for wind speed quantiles above the 70th percentile, with trends as high as $0.3 \pm 0.09 \text{ m s}^{-1} \text{ yr}^{-1}$ (s.e.) for the strongest cyclones. We note separate upward trends in the estimated lifetime-maximum wind speeds of the very strongest tropical cyclones (99th percentile) over each ocean basin, with the largest increase at this quantile occurring over the North Atlantic, although not all basins show statistically significant increases. Our results are qualitatively consistent with the hypothesis that as the seas warm, the ocean has more energy to convert to tropical cyclone wind.

An important concern about the consequences of climate change is the potential increase in tropical cyclone activity. Theoretical arguments^{5,6} and modelling studies^{7,8} indicate that tropical cyclone winds should increase with increasing ocean temperature. Direct observational verification of this relationship over the global tropics is lacking, but Atlantic sea surface temperature (SST), which is correlated with global mean near-surface air temperature, helps explain¹ the recent upswing in frequency and intensity of Atlantic tropical cyclones. However, it has been argued that the data are not reliable enough to make assertions about the relationship between climate change and hurricanes^{9–13} and that the correlation may involve both regional and remote SSTs^{14,15}. Here we shed new light on this topic by using globally consistent satellite-derived tropical cyclone wind speeds¹⁶ and by focusing on the lifetime-maximum wind speeds of the strongest tropical cyclones each year.

Figure 1a shows the satellite-derived lifetime-maximum wind speeds grouped by year over the period 1981–2006, displayed as box plots (see Supplementary Information). The number of cyclones per year over the globe is shown above the time axis; there is no trend in these counts. Also, there is no trend in the median lifetime-maximum wind speed, as shown by the nearly horizontal red line, which is the best-fit line through the annual 50th-percentile values (black dashes inside the boxes). However at cyclone wind speeds above the median, upward trends are noted. Thus, the upper-quartile value (top of the box) is increasing (green line) and so are higher quantile values (for example the top of the vertical dashed line), where the upward trends are more pronounced.

To quantify and determine the significance of these trends, we use quantile regression. Quantile regression as employed here is a method to estimate the change (trend) in lifetime-maximum wind speed quantile as a function of year. A quantile is a point taken from

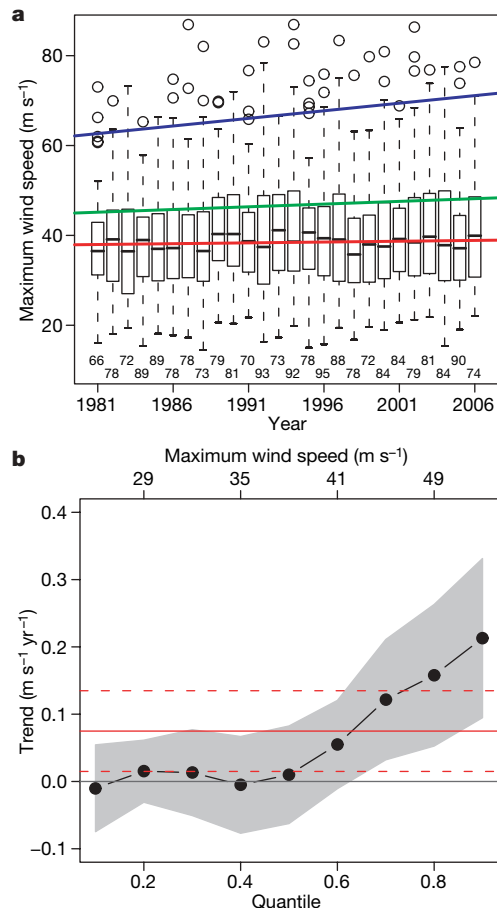


Figure 1 | Analysis and model results of satellite-derived tropical cyclone lifetime-maximum wind speeds. **a**, Box plots by year. Trend lines are shown for the median, 0.75 quantile, and 1.5 times the interquartile range. **b**, Trends in global satellite-derived tropical cyclone maximum wind speeds by quantile, from 0.1 to 0.9 in increments of 0.1. Trends are estimated coefficients from quantile regression in units of metres per second per year. The point-wise 90% confidence band is shown in grey, under the assumption that the errors are independent and identically distributed. The solid red line is the trend from a least-squares regression of wind speed as a function of year and the dashed red lines delineate the 90% point-wise confidence band about this trend.

¹Department of Geography, Florida State University, Tallahassee, Florida 32306, USA. ²Cooperative Institute for Meteorological Satellite Studies, University of Wisconsin–Madison, Madison, Wisconsin 53706, USA.

the inverse cumulative distribution function of the set of wind speeds so that, for example, the 0.7 quantile is the value such that 70% of the tropical cyclones have lifetime-maximum wind speeds below this value (70th percentile).

Figure 1b shows global trends in tropical cyclone lifetime-maximum wind speeds for selected quantiles. Trends are near zero for the lower quantiles (median and below), but are upward for the higher quantiles, with the largest trends noted for the highest quantile (90th percentile). The shading shows the 90% point-wise confidence band about these trend estimates. Trends significantly above zero are seen for quantiles above 0.7. The maximum wind speeds over the entire period of record corresponding to the selected quantiles are also displayed. For comparison, the red lines are from a least-squares regression of maximum wind speed as a function of year, with the solid line showing the trend of the mean lifetime-maximum wind speed and the dashed lines indicating the 90% confidence limits about this trend. We note that the trend value of approximately $0.15 \text{ m s}^{-1} \text{ yr}^{-1}$ interpolated from Fig. 1b at the 75th percentile matches the slope value of the trend line corresponding to the upper quantiles shown as the green line in Fig. 1a. The results clearly show that the strongest tropical cyclones are getting stronger.

To examine whether these global increases are the result of trends occurring in one or two tropical cyclone basins, we use quantile regression to model the satellite-derived wind speeds from each basin separately (Fig. 2). With the exception of the South Pacific Ocean, all tropical cyclone basins show increases in the lifetime-maximum wind speeds of the strongest storms. The increases are greatest for cyclones over the North Atlantic and northern Indian oceans. Consistent with earlier results, only over the North Atlantic is there a significant increase in average tropical cyclone intensity. The width of the confidence interval is inversely proportional to the number of cyclones and proportional to the variability in wind speeds. We

display trends and associated standard errors and *P* values for upper-quantile (≥ 85 th-percentile) lifetime-maximum wind speeds in Table 1. We note significant ($P < 0.05$) increases for at least one quantile level in all six basins, and upward trends in the wind speeds of the strongest tropical cyclones in all basins for the highest quantile considered (99th percentile), although not all trends at this extreme quantile are statistically significant.

The potential intensity of a tropical cyclone is directly related to SST below the cyclone, all else being equal^{5,6,17,18}. Because the strongest cyclones at their maxima are, on average, closest to their maximum potential intensities, increases in observed maximum wind speeds should occur with SST at the upper quantiles. To test this, we averaged Hadley Centre¹⁹ SST data over each of the six tropical cyclone basins during the peak months of their respective tropical cyclone seasons. The basin means are then averaged to obtain a global tropics SST value for each year over the period 1981–2006. These values are subsequently used instead of year in the quantile regression. The results are shown in Fig. 3a. Consistent with the theory, the trends in units of metres per second per degree Celsius are positive for the upper quantiles. For a 1°C rise in SST, the results show an increase of $1.9 \pm 2.9 \text{ m s}^{-1}$ (s.e.) in the value of the 80th percentile and $6.5 \pm 4.2 \text{ m s}^{-1}$ in the value of the 90th percentile.

Table 1 | Summary statistics

Statistic	Quantile				
	0.85	0.90	0.95	0.975	0.99
Global (2,097)					
<i>W</i> (m s^{-1})	51.9	55.8	62.6	68.8	75.9
Trend ($\text{m s}^{-1} \text{ yr}^{-1}$)	+0.19	+0.21	+0.18	+0.25	+0.30
s.e. ($\text{m s}^{-1} \text{ yr}^{-1}$)	0.049	0.072	0.141	0.122	0.093
<i>P</i>	<0.001	0.003	0.212	0.044	0.001
Western North Pacific (698)					
<i>W</i> (m s^{-1})	58.9	63.7	69.6	73.1	77.6
Trend ($\text{m s}^{-1} \text{ yr}^{-1}$)	+0.12	+0.14	+0.09	+0.29	+0.36
s.e. ($\text{m s}^{-1} \text{ yr}^{-1}$)	0.190	0.177	0.192	0.116	0.230
<i>P</i>	0.520	0.434	0.647	0.012	0.115
Eastern North Pacific (423)					
<i>W</i> (m s^{-1})	44.8	48.8	53.0	57.3	62.8
Trend ($\text{m s}^{-1} \text{ yr}^{-1}$)	+0.11	+0.16	+0.33	+0.46	+0.80
s.e. ($\text{m s}^{-1} \text{ yr}^{-1}$)	0.117	0.156	0.160	0.184	NA
<i>P</i>	0.327	0.308	0.042	0.014	NA
Southern Indian (413)					
<i>W</i> (m s^{-1})	49.2	51.3	56.4	57.8	62.6
Trend ($\text{m s}^{-1} \text{ yr}^{-1}$)	+0.28	+0.29	+0.44	+0.43	+0.69
s.e. ($\text{m s}^{-1} \text{ yr}^{-1}$)	0.065	0.145	0.177	0.178	0.353
<i>P</i>	<0.001	0.046	0.014	0.016	0.052
North Atlantic (291)					
<i>W</i> (m s^{-1})	48.9	54.8	60.3	72.7	77.8
Trend ($\text{m s}^{-1} \text{ yr}^{-1}$)	+0.63	+0.73	+0.81	+1.11	+1.52
s.e. ($\text{m s}^{-1} \text{ yr}^{-1}$)	0.228	0.226	0.449	0.356	NA
<i>P</i>	0.006	0.001	0.073	0.002	NA
South Pacific (157)					
<i>W</i> (m s^{-1})	52.8	54.7	59.8	65.8	67.1
Trend ($\text{m s}^{-1} \text{ yr}^{-1}$)	-0.04	-0.23	-0.37	-0.06	+0.46
s.e. ($\text{m s}^{-1} \text{ yr}^{-1}$)	0.174	0.227	0.214	0.563	0.210
<i>P</i>	0.803	0.313	0.088	0.914	0.030
Northern Indian (115)					
<i>W</i> (m s^{-1})	41.5	45.0	47.4	50.4	56.4
Trend ($\text{m s}^{-1} \text{ yr}^{-1}$)	+0.48	+0.42	+0.69	+0.83	+0.87
s.e. ($\text{m s}^{-1} \text{ yr}^{-1}$)	0.224	0.220	0.222	NA	NA
<i>P</i>	0.034	0.059	0.002	NA	NA

Statistics are from a quantile regression of lifetime-maximum tropical cyclone wind speed (derived from satellites) as a function of year, either globally or by tropical cyclone basin. Sample size (number of tropical cyclones) is given in parentheses next to the basin name. Values are shown for selected upper quantiles (0.85, 0.90, 0.95, 0.975, and 0.99). For each quantile, *W* denotes the tropical cyclone lifetime-maximum wind speed over all cyclones in the basin and over all years in the analysis (1981–2006). For some extreme quantiles the s.e., computed assuming independent and identically distributed errors, and *P* value are not reliable and so are reported as not available (NA).

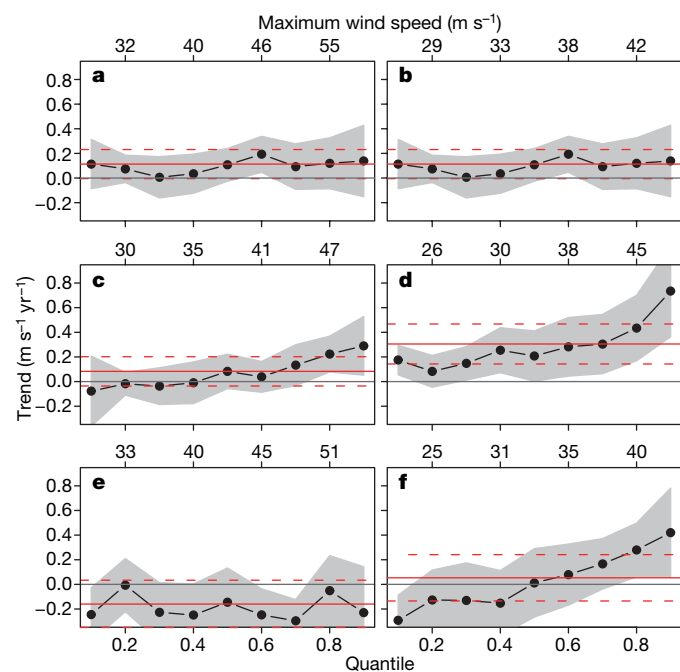


Figure 2 | Trends in satellite-derived tropical cyclone lifetime-maximum wind speeds from quantile regression. **a**, Western North Pacific Ocean cyclones (cyclone count, 698); **b**, eastern North Pacific Ocean cyclones (423); **c**, southern Indian Ocean cyclones (413); **d**, North Atlantic Ocean cyclones (291); **e**, South Pacific Ocean cyclones (157); **f**, northern Indian Ocean cyclones (115). The point-wise 90% confidence band is shown in grey, under the assumption that the errors are independent and identically distributed. Each solid red line is the trend from a least-squares regression of wind speed as a function of year and the dashed red lines delineate the 90% point-wise confidence band about this trend.

Upward trends can be interpreted as an increase in the number of cyclones exceeding a threshold quantile. For example, at the 80th percentile, on average 17 cyclones globally exceed 49 m s^{-1} . With a 1°C rise in SST, the 80th percentile increases to 51 m s^{-1} . At this threshold level, on average 13 cyclones per year are observed. So the increase in SST of 1°C results in an increase in the global frequency of strong cyclones from 13 to 17 cyclones (31%) per year. The best estimates indicate that the strongest tropical cyclones are getting stronger with increasing SST, but the uncertainty ranges are relatively large. The relationship does not imply causality and is not directly comparable to results from numerical models with forced SST changes. We make no attempt here to control other factors probably related to intense tropical storminess such as changes in region of origin, cyclone duration, El Niño conditions and solar activity.

For comparison, we repeat the quantile regression for the set of lifetime-maximum wind speeds based on the global best-track data sets (Fig. 3b). The best-track data represent a best estimate of cyclone position and intensity from all available information. Results are similar, showing an increase in lifetime-maximum wind speed per degree Celsius for the set of strongest cyclones but not for the set of weaker cyclones. Magnitudes of the change are not directly comparable, because the variance of the satellite-derived wind speeds is, by construction (regression model), less than observed wind speeds, which results in a mismatch in the quantile values. Moreover, inhomogeneities in the best-track data due to changes in the availability

and quality of information over time probably contribute to the magnitude of this trend.

Recent results from the analyses of global tropical cyclone trends have been questioned owing to a lack of consensus regarding the reliability of the data. Moreover, results have not been matched to theory, because the focus was on a change in mean tropical cyclone statistics. In contrast, the results presented here are conclusive in showing significant increasing trends in the satellite-derived lifetime-maximum wind speeds of the strongest tropical cyclones globally, and are qualitatively consistent with the heat-engine theory of cyclone intensity. Thus, as seas warm, the ocean has more energy that can be converted to tropical cyclone wind.

Regional differences in the magnitude of the upward trends are possibly due in part to the rate of warming relative to the existing warmth in the basin. Relatively cooler basins with large SST increases should therefore show the greatest upward trends in the intensity of the strongest tropical cyclones. The three coolest basins over the period 1981–2006 are the North Atlantic (27.6°C), the eastern North Pacific (27.9°C) and the southern Indian (27.5°C), and the rates of warming in these basins are respectively $0.69 \pm 0.18^\circ\text{C}$, $0.33 \pm 0.24^\circ\text{C}$ and $0.21 \pm 0.16^\circ\text{C}$ per 30 years. These basins show corresponding upward trends at the 99th percentile of 1.52, 0.80 and $0.69 \text{ m s}^{-1} \text{ }^\circ\text{C}^{-1}$, respectively. Small positive correlations are noted between the warming trends in the tropical oceans and the upward trends in the intensity of the strongest tropical cyclones, using all six basins, with the largest correlation ($r = 0.47$, $N = 6$) occurring for the 99th-percentile trends. It is necessary to control other factors such as changes in upper-tropospheric temperatures, shearing winds and proximity to land to better understand regional differences in these trends.

METHODS SUMMARY

We use log-linear regression to model the lifetime maximum wind speeds using principal components of brightness temperature profiles from satellite imagery^{20–24} for 171 tropical cyclones over the North Atlantic Ocean. The regression model is modified from ref. 16 to better account for the skewness in wind speed values. Model details and diagnostics are given in the Supplementary Information. We apply the regression model to satellite imagery for 2,097 tropical cyclones around the globe over the period 1981–2006 to produce the satellite-derived per-cyclone lifetime-maximum wind speeds.

We subsequently estimate trends in satellite-derived lifetime-maximum wind speeds using quantile regression. Quantile regression extends ordinary least-squares regression to conditional quantiles of the response variable²⁵ (lifetime-maximum wind speed). Quantiles are values taken at regular intervals from the cumulative distribution function. The quantiles divide a set of ordered wind speeds into equally sized subsets. A minimization procedure determines the quantile regression trend. More details on quantile regression are given in the Supplementary Information. All statistics are performed using the software environment R (<http://www.r-project.org>) and the quantile regression package `quantreg` (R package version 4.17; <http://www.r-project.org>).

Received 25 January; accepted 27 June 2008.

- Emanuel, K. A. Increasing destructiveness of tropical cyclones over the past 30 years. *Nature* **436**, 686–688 (2005).
- Webster, P. J., Holland, G. J., Curry, J. A. & Chang, H. R. Changes in tropical cyclone number, duration, and intensity in a warming environment. *Science* **309**, 1844–1846 (2005).
- Trenberth, K. Uncertainty in hurricanes and global warming. *Science* **308**, 1753–1754 (2005).
- Elsner, J. B. Granger causality and Atlantic hurricanes. *Tellus* **59A**, 476–485 (2007).
- Emanuel, K. A. The theory of hurricanes. *Annu. Rev. Fluid Mech.* **23**, 179–196 (1991).
- Holland, G. J. The maximum potential intensity of tropical cyclones. *J. Atmos. Sci.* **54**, 2519–2541 (1997).
- Knutson, T. R. & Tuleya, R. E. Impact of CO_2 -induced warming on simulated hurricane intensity and precipitation: Sensitivity to the choice of climate model and convective parameterization. *J. Clim.* **17**, 3477–3495 (2004).
- Bengtsson, L. *et al.* How may tropical cyclones change in a warmer climate. *Tellus* **59A**, 539–561 (2007).
- Pielke, R. A. Jr, Landsea, C., Mayeld, M., Laver, J. & Pasch, R. Hurricanes and global warming. *Bull. Am. Meteorol. Soc.* **86**, 1571–1575 (2005).

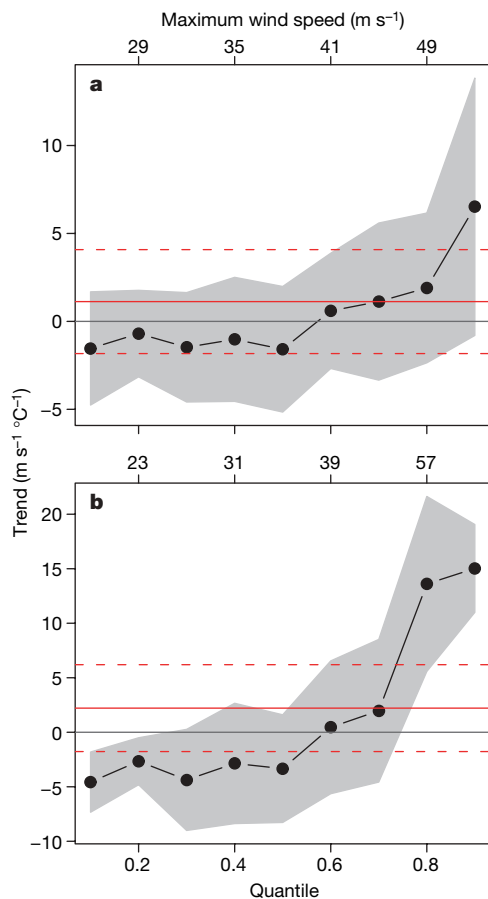


Figure 3 | Quantile regression of tropical cyclone lifetime-maximum wind speed on globally averaged tropical storm basin SST. **a**, Plotted using satellite-derived maximum wind speeds; **b**, plotted using maximum wind speeds as recorded in the best-track observational archives. The point-wise 90% confidence band is shown in grey under the assumption that the errors are independent and identically distributed. Each solid red line is the trend from a least-squares regression of wind speed as a function of year and the dashed red lines delineate the 90% point-wise confidence band about this trend.

10. Landsea, C. W. Hurricanes and global warming. *Nature* **438**, E11–E13 (2005).
11. Chan, J. C. L. Comment on "Changes in tropical cyclone number, duration, and intensity in a warming environment". *Science* **311**, 1713 (2006).
12. Klotzbach, P. J. Trends in global tropical cyclone activity over the past twenty years (1986–2005). *Geophys. Res. Lett.* **33**, doi:10.1029/2006GL025881 (2006).
13. Landsea, C. W., Harper, B. A., Hoarau, K. & Knaff, J. A. Can we detect trends in extreme tropical cyclones? *Science* **313**, 452–454 (2006).
14. Vecchi, G. A. & Soden, B. J. Effect of remote sea surface temperature change on tropical cyclone potential intensity. *Nature* **450**, 1066–1070 (2007).
15. Swanson, K. L. Nonlocality of Atlantic tropical cyclone intensities. *Geochem. Geophys. Geosyst.* **9**, doi:10.1029/2007GC001844 (2008).
16. Kossin, J. P., Knapp, K. R., Vimont, D. J., Murnane, R. J. & Harper, B. A. A globally consistent reanalysis of hurricane variability and trends. *Geophys. Res. Lett.* **34**, doi:10.1029/2006GL028836 (2007).
17. Shen, W., Tuleya, R. E. & Ginis, I. A sensitivity study of the thermodynamic environment on GFDL model hurricane intensity: Implications for global warming. *J. Clim.* **13**, 109–121 (2000).
18. Bister, M. & Emanuel, K. A. Low frequency variability of tropical cyclone potential intensity. 1. Interannual to interdecadal variability. *J. Geophys. Res.* **107**, doi:10.1029/2001JD000776 (2002).
19. Rayner, N. A. *et al.* Global analysis of sea surface temperature, sea ice, and night marine air temperature since the late nineteenth century. *J. Geophys. Res.* **108**, doi:10.1029/2002JD002670 (2003).
20. Knapp, K. R. Calibration assessment of ISCCP geostationary infrared observations using HIRS. *J. Atmos. Oceanic Technol.* **25**, 183–195 (2008).
21. Knapp, K. R. & Kossin, J. P. A new global tropical cyclone data set from ISCCP B1 geostationary satellite observations. *J. Appl. Remote Sensing* **1**, 013505 (2007).
22. Knapp, K. R., Bates, J. J. & Barkstrom, B. Scientific data stewardship: Lessons learned from a satellite-data rescue effort. *Bull. Am. Meteorol. Soc.* **88**, 1359–1361 (2007).
23. Franklin, J. L., Black, M. L. & Valde, K. GPS dropwindsonde wind profiles in hurricanes and their operational implications. *Weather Forecast.* **18**, 32–44 (2003).
24. Gunshor, M. M., Schmit, T. J. & Menzel, W. P. Intercalibration of the infrared window and water vapor channels on operational geostationary environmental satellites using a single polar-orbiting satellite. *J. Atmos. Oceanic Technol.* **21**, 61–68 (2004).
25. Yu, K., Lu, Z. & Stander, J. Quantile regression: applications and current research areas. *Statistician* **52**, 331–350 (2003).

Supplementary Information is linked to the online version of the paper at www.nature.com/nature.

Acknowledgements The work was supported by the US National Science Foundation (ATM-0738172 and ATM-0614812) and by the Risk Prediction Initiative of the Bermuda Institute for Ocean Studies (RPIO6-3-001).

Author Information Reprints and permissions information is available at www.nature.com/reprints. Correspondence and requests for materials should be addressed to J.B.E. (jelsner@fsu.edu).